Electric-field-induced dielectric and temperature changes in a ⟨011⟩-oriented $Pb(Mg_{1/3}Nb_{2/3})O_3$-$PbTiO_3$ single crystal

J. Peräntie, J. Hagberg, A. Uusimäki, and H. Jantunen
Microelectronics and Materials Physics Laboratories, University of Oulu, P.O. Box 4500, FIN-90014 Oulu, Finland
(Received 4 August 2010; revised manuscript received 4 October 2010; published 21 October 2010)

Dielectric and direct temperature changes induced by an electric field were investigated in a ⟨011⟩-oriented $0.72Pb(Mg_{1/3}Nb_{2/3})O_3$-$0.28PbTiO_3$ single crystal as a function of temperature. Field-induced temperature changes were measured directly from the surface of the crystal by a thermocouple. Three distinct anomalies at temperatures of ~68, ~96, and ~128 °C were identified in the dielectric and temperature change responses of the crystal, dividing the temperature range into four distinct phase stability regions with different field-induced behaviors. Just above the depolarization temperature of 128 °C, dielectric hysteresis showed a double-loop nature caused by a reversible nonpolar-polar phase transition accompanied by an increase in the electrocaloric temperature change. Two other reversible field-induced phase transitions with different field-induced thermal behaviors were evidenced in the polarization and temperature responses in the temperature ranges of 96–128 °C and below 68 °C.

DOI: 10.1103/PhysRevB.82.134119 PACS number(s): 77.80.B−, 77.70.+a, 77.84.Ek, 77.22.Ej

I. INTRODUCTION

Observations of extraordinary piezoelectric responses in the nonpolar directions in poled rhombohedral ferroelectric $Pb(Zr_{1-x}Ti_x)O_3$ (Refs. 1 and 2) as well as in related relaxor-based $(1-x)Pb(Mg_{1/3}Nb_{2/3})O_3$-$xPbTiO_3$ (PMN-PT) and $(1-x)Pb(Zn_{1/3}Nb_{2/3})O_3$-$xPbTiO_3$ (PZN-PT) solid solution systems near the morphotropic phase boundary (MPB) (Refs. 3 and 4) has led to increasing research efforts focusing on these types of materials. In particular, discoveries[5–9] and predictions[10,11] of monoclinic M_A, M_B, and M_C phases and their function as structural bridges[12] between higher symmetry rhombohedral, orthorhombic, and tetragonal phases in these materials have provided new perspectives for a better understanding of the reasons behind the abnormal electromechanical behavior. A remarkable breakthrough came with the polarization rotation model, which was developed for $BaTiO_3$ by means of first-principles calculations.[13] The model explains the high electromechanical response in rhombohedral crystals along the nonpolar [001] axis by the field-induced polarization rotation in the plane defined by pseudocubic directions [001] and [111]. This plane corresponds to the earlier case where the monoclinic phase has a mirror plane but no symmetry axis, and thus it acts as a bridging phase between the rhombohedral and tetragonal phases.[14] However, there are other arguments[15,16] that monoclinic symmetry is not a direct indication or necessity that the extraordinary piezoelectric properties can be understood by polarization rotation. In the end, the observed monoclinic symmetry and large piezoelectric response are believed to be closely linked[17] but clearly more studies are needed to complete the picture related to this topic.

Although extensive research and attention has been paid to these technologically important materials, even the phase diagram of the PMN-PT system under the effect of an electric field is far from being clear or fully characterized, since it has been proven very complex, especially close to the MPB but even with lower PT concentrations. Due to the great complexity and hierarchy of polydomain patterns, the observed effective macroscopic symmetry can be very different from the crystal symmetry.[18] Also, the true nature and stability of the intermediate monoclinic and orthorhombic phases are still unclear.[17] For example, one approach is to describe the monoclinic phases as distortions induced by residual fields from parental phases instead of being true phases.[15,17,19] Furthermore, it has been predicted and demonstrated that monoclinic as well as orthorhombic phases observed at the macroscopic level are actually adaptive phases composed of T or R nanodomains.[20–25] Additionally, the coexistence of two or more phases as well as coexisting polar nanodomains and microdomains have been evidenced, especially in unpoled crystal states of PMN-PT.[26–29] The poling process usually removes any phase coexistences, and leaves a domain-engineered single phase structure.[17] The poling treatment required for enhanced piezoelectricity is commonly referred to as domain engineering in which a sufficiently large electric field applied in the nonpolar direction creates a set of domains where polarizations are oriented so that their angles to the poling direction are minimized.[30] And besides this, as Cao *et al.*[31] demonstrated in their work, zero-field phase stability after poling is very fragile in the PMN-PT system, where the phase structure is highly dependent on the composition, crystal orientation, and acting electric-field strength during the field-cooling routine.

Moreover, in many important solid-state phenomena, including a startling converse piezoelectric effect, the basic operation takes place more or less at a constant temperature, and the driving electric field is altered. With this viewpoint in mind, field-induced phase transitions and structural changes at constant temperatures have different characteristics than the widely studied changes induced by more conventional means of cooling and heating with a constant electric field, and thus they should be reviewed and treated separately.[32–34] To date, field-induced $R \rightarrow M_A \rightarrow T$ or $R \rightarrow M_A \rightarrow M_C \rightarrow T$ phase transitions found close to the morphotropic phase boundary in ⟨001⟩-oriented PMN-PT and PZN-PT have been emphasized due to their relation to high piezoelectric response.[35,36] However, enhanced piezoelectricity can also be

obtained in ⟨011⟩-oriented PZN-PT as well as PMN-PT studied herein, where the orthorhombic phase can be induced by an electric field.[37,38]

Besides being a straightforward method for direct evaluation of the electrocaloric effect, which is a general tendency of dielectrics to reversibly change their temperature in adiabatic conditions with an applied electric field,[39] field-induced temperature change measurement provides additional information about phase transitions in materials.[40] Although PMN-PT and other relaxor-based materials have been considered for electrocaloric purposes with promising results,[41,42] on the other hand experimentally observed field-induced temperature changes in these crystals have not been investigated very much. In many studies the material's electrocaloric temperature change is predicted indirectly from dielectric polarization measurements as a function of temperature and the electric field, using the thermodynamic equation[39]

$$\Delta T = -\frac{T}{C_E}\int_{E_1}^{E_2}\left(\frac{\partial P}{\partial T}\right)_E dE, \tag{1}$$

where C_E is the heat capacity per unit volume in a constant electric field (E), P is the polarization, and T is the absolute temperature. The direct temperature and calorimetric measurements performed so far in PMN-based materials[43–45] show variable results, and it is hard to draw any far-reaching conclusions about their electrocaloric behavior. With direct temperature measurement it is possible to obtain more detailed information on the electrocaloric effect.

This paper reports electric-field-induced dielectric and temperature change behavior at constant temperatures in ⟨011⟩-oriented 72%$Pb(Mg_{1/3}Nb_{2/3})O_3$-28%$PbTiO_3$ (PMN-28PT). The observed induced changes are attributed to the formation of domain-engineered states as well as field- and temperature-induced phase transitions. The measured temperature changes in adiabatic conditions allowed observation of the heat contents and thermal characteristics of the field-induced phase transitions.

II. EXPERIMENTAL

PMN-28PT single crystals in a ⟨011⟩ orientation, with sputtered Cr/Au electrodes on the (011) faces, 1 mm in thickness and grown with the Bridgman technique, were acquired from TRS Technologies, Inc. (State College, PA). Dielectric permittivity measurements were performed with a HP/Agilent 4284A precision *LCR* meter with zero-field heating/cooling (ZFH/ZFC) from prepoled and unpoled states. An electric-field pulse was provided with an Agilent 33120A function generator connected via a Radiant RT6000HVA voltage amplifier. Dielectric polarization current through a shunt resistor in response to a triangle wave was measured with an Agilent 34411A multimeter. For direct temperature measurements, the crystal was mounted on a customized sample holder through thin metallic wires with 3M polyimide adhesive tape. Temperature response was measured with an Agilent 34420A through a chromel-alumel thermocouple attached to one side of the sample. In all direct temperature measurements of the sample, the electric-field stimulus was a 6 s rectangular pulse applied separately for each electric-field strength. The sample construction was closed inside a glass beaker to minimize thermal variation and ensure a sufficiently long thermal time constant in comparison to the measurement cycle used. Before each polarization measurement the crystal was depolarized at 180 °C. Temperature dependence measurements were performed using ESPEC BTZ175E and Memmert UFP400 ovens.

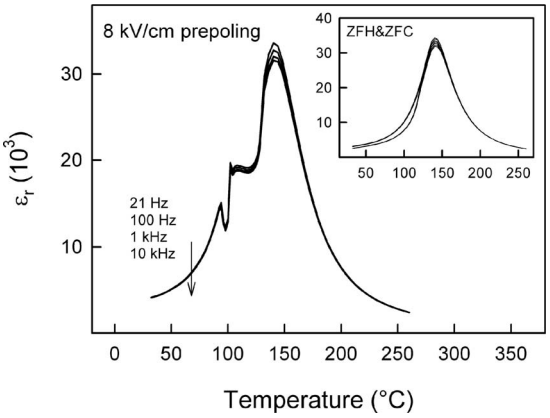

FIG. 1. Temperature dependence of the relative permittivity of the poled ⟨011⟩-oriented PMN-28PT single crystal upon heating at 21 Hz, 100 Hz, 1 kHz, and 10 kHz. The inset shows the temperature dependence of the relative permittivity of the unpoled sample upon zero-field heating and cooling.

III. RESULTS AND DISCUSSION

A. Dielectric permittivity

Figure 1 shows the relative permittivity of the ⟨011⟩-oriented PMN-28PT crystal as a function of temperature measured with and without room-temperature prepoling. The maximum of the relative permittivity peak is located at T_m=140 °C, which seems to be systematically higher than in other studies.[46,47] However, there is significant variance in the reported single-crystal material properties, and especially in the transition temperatures of nominally similar PMN-PT compositions.[48] This variance can arise from differences in real composition and measurement methods, defects induced by different single-crystal growth methods, and even from misinterpretation or mixing up of distinct characteristic temperatures.[28,48,49] For this reason, references and comparisons to other studies on the grounds of nominal compositions should be done with extreme care.

The inset of Fig. 1 shows that there is small hysteresis behavior with ZFH/ZFC of the unpoled crystal measured at 21 Hz–10 kHz, and the related permittivity values diverge below a temperature of 126 °C. This indicates a first-order phase transition between the microdomain relaxor and macrodomain ferroelectric states since there was no frequency dispersion present below the mentioned temperature. A characteristic relaxor behavior with strong frequency dispersion was observed close to the temperature of maximum permittivity, T_m. Upon zero-field cooling, a successive structural

phase transition sequence, cubic→tetragonal →rhombohedral, has been evidenced in a wide composition region of $x=25-35$ % in PMN-xPT ceramics.[46] In contrast, in single-crystal PMN-xPT, the tetragonal phase was found to be present only for $x \geq 30\%$, and a cubic →rhombohedric sequence was found upon zero-field cooling for $x<30\%$.[31]

Prepoling of the crystal with a strong enough electric field (≥2 kV/cm) at room temperature led to increased permittivity, which suggests that a ferroelectric rhombohedral order was enhanced in the crystal.[50] Sufficient electric poling of the rhombohedral state crystal in the nonpolar ⟨011⟩ direction (or ⟨001⟩ direction) creates engineered multidomain states with enhanced piezoelectric properties, where two (or four) degenerate states out of eight possible ⟨111⟩-directed spontaneous polarization states are stabilized.[4,51] During zero-field heating, the relative permittivity of the sample prepoled with 8 kV/cm experienced two additional distinct changes at temperatures of 94 and 102 °C, independent of the frequency. Similar peaks have also been observed in poled ⟨110⟩-oriented PMN-29PT and PMN-30PT single crystals. The first peak is associated with a phase transition to the orthorhombic phase while the second peak is attributed to a phase transition from the ferroelectric orthorhombic phase to the ferroelectric tetragonal phase.[50,52,53] Above the temperature of the second peak there is some small frequency dispersion in permittivity, which suggests that some degree of relaxor microdomain state appears instead of a fully macroscopic tetragonal order. Finally, around 128 °C permittivity increases rapidly due to macroscopic depolarization of the crystal, and the dispersion behavior strengthens when moving toward T_m. Here it appears that the determined depoling temperature T_{dp} of 126 °C (from the ZFH/ZFC procedure, inset of Fig. 1) and 128 °C (from the prepoling/ZFH procedure, Fig. 1) are in good accordance with Ref. 54, and as expected for relaxor ferroelectrics, they reside significantly lower than the temperature of maximum permittivity, $T_m=140$ °C.

B. Dielectric polarization and hysteresis

Field-induced phase and polarization changes at constant temperatures, in which also the electrocaloric temperature change can be classified, have different characteristics than thermally induced changes with a constant electric field in relaxor-based materials.[32–34] To study the isothermal field-induced changes, dielectric polarization measurements with a maximum electric field of 9 kV/cm at 1 Hz were performed at constant temperatures. In order to also record the virgin polarization curve, before each measurement the crystal was first forced into a depoled state by annealing at 180 °C for 10 min. The remanent polarizations P_r and coercive electric fields E_c extracted from the measured hysteresis loops are shown as a function of temperature in Fig. 2. Four different temperature ranges, where both remanent polarization and coercive field are clearly different, can be distinguished from the figure. Above 128 °C the remanent polarization and coercive field show relatively small values, but below this temperature a significant increase in both values is observed

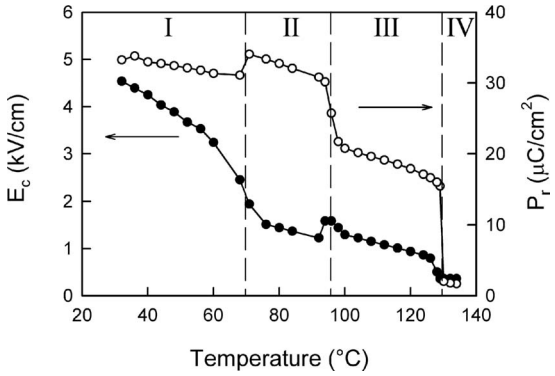

FIG. 2. Coercive electric field and remanent polarization as a function of temperature in ⟨011⟩-oriented PMN-28PT.

when the crystal becomes macroscopically ferroelectric. When the temperature is decreased, two more abrupt changes can be seen, starting from temperatures of 98 °C and 68 °C, respectively. Between these temperatures, remanent polarization is locally increased and the coercive electric field is decreased.

The four observed temperature ranges, I–IV, with different remanent polarization and coercive electric-field values in Fig. 2 refer to different phase stability ranges in the poled PMN-28PT single crystal. Hysteresis loops representing the typical polarization properties of each characteristic temperature range are plotted in Fig. 3. The first hysteresis curve taken at 52 °C represents temperature range I, which extends down to room temperature. Within this range at 52 °C two distinct changes in the virgin polarization curves are found with electric fields of 1.95 and 4.9 kV/cm. The first one is caused by the initial poling of the sample and the second one is an indication of a field-induced phase transition. By further tracing the polarization curve to the descending electric-field step, it can be seen that the sudden polarization change due to the field-induced phase transition is reversible in nature, showing a clear hysteretic behavior with a lower back-

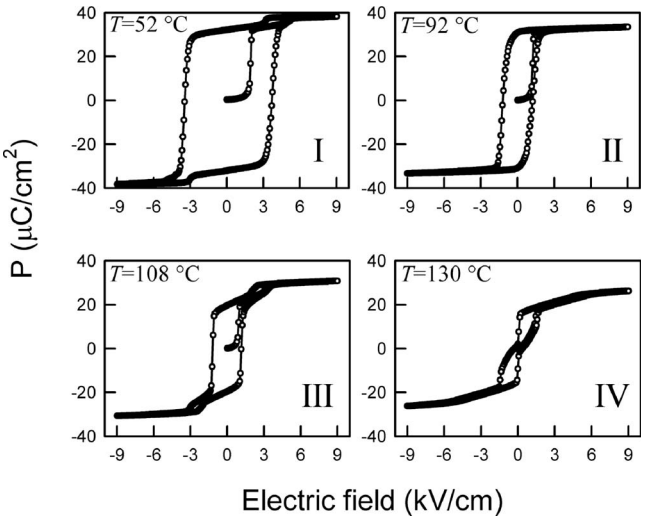

FIG. 3. Series of dielectric hysteresis loops in ⟨011⟩-oriented PMN-28PT, each taken at distinct temperatures after zero-field cooling from 180 °C.

inducing field of 3.2 kV/cm in the descending electric-field phase.

The observed changes point to a rhombohedral-orthorhombic phase transition, which is effectively related to a combination of partial rotation and discontinuous jump of polarization from ⟨111⟩ to ⟨110⟩, and has been evidenced previously at room temperature by means of structural, strain, and polarization measurements for PMN-PT (Refs. 8, 55, and 56) and PZN-PT (Ref. 57) with an electric field along ⟨110⟩. With higher PT contents of 32 and 33 mol %, this phase transformation changes from reversible to irreversible in nature and the orthorhombic phase is stable after removal of the electric field, causing degradation in piezoelectric properties.[56,58] It is thought that this phase transformation advances gradually via an intermediate monoclinic M_B phase, which has been found in ⟨110⟩-oriented PMN-PT and PZN-PT, and is consistent with the developed thermodynamic theory.[8,10,59,60] Actually, the phase transition sequence $R \rightarrow M_B \rightarrow O$ is not fully reversible, and the monoclinic phase or distortion instead of the rhombohedral is found to recover after removal of the electric field in PMN-30PT.[8]

In the second polarization curve in Fig. 3, measured at 92 °C and representing temperature range II, remanent polarization is increased and the coercive field is decreased, making the hysteresis loop a slim and well-defined curve whose polarization saturates early with $E=1.22$ kV/cm. Additionally, it was noted that due to the initial poling, the relative permittivity of the crystal decreased sharply in temperature range II while it increased in the other characteristic temperature ranges, I and III. This decrease in permittivity is more a sign of monodomain formation or a possible phase transition since the permittivity of an otherwise formed domain engineered state is usually increased, as found in Fig. 1, and is expected to be much larger than that of a monodomain sample.[48] Similar decreased permittivity after sufficient poling treatment in the ⟨110⟩ direction at room temperature is found in PMN-xPT crystals with higher x, and it has been attributed to the inducement of a monodomain orthorhombic ferroelectric phase.[37,53] At 92 °C no further anomalous behavior in polarization was detected up to 9 kV/cm with either an increasing or decreasing electric field.

The shape of the hysteresis loop at 108 °C (in temperature range III) resembles the first one taken at 52 °C (in temperature range I) since it has very similar distinct and reversible changes in polarization at certain electric-field strengths. The fourth hysteresis loop at 130 °C (in temperature range IV) presents the characteristics of the temperature range located just above the temperature where crystal loses a majority of its remanent polarization. Here, the shape of the hysteresis loop is reminiscent of a double loop, which indicates a field-induced metastable ferroelectric phase at slightly higher temperatures than the depolarization temperature.[61,62]

Field-induced polarization changes are presented in more detail in Fig. 4 for temperatures of 52 °C (range I) and 108 °C (range III). Here the aforementioned abrupt changes in polarization can be clearly identified, and it can be seen that the second change in polarization at 52 °C actually consists of two distinct changes close to each other. This kind of stepwise change in polarization behavior was present only in lower phase transition temperature range I, with an increasing field associated with a $M_B \rightarrow O$ transition, and it recurred in the opposite direction after reversal of the polarization.

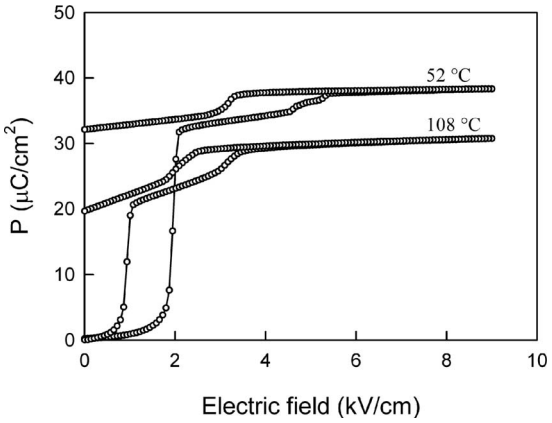

FIG. 4. Polarization behavior from a virgin state of ⟨011⟩-oriented PMN-28PT at 52 °C and 108 °C after zero-field cooling from 180 °C.

All the observed threshold electric fields that cause rapid polarization changes were determined from the maximum of differential $\partial P/\partial E$, and they are collectively presented in Fig. 5 as a function of temperature. The first polarization changes from the depoled virgin state due to sample poling are depicted as black triangles. Black circles indicate the threshold fields of reversible polarization changes with an increasing field starting from the virgin state after zero-field cooling, and white circles indicate the threshold field of reversible polarization changes extracted with a decreasing field. The aforementioned temperature ranges, I–IV, for phase stabilities are easily distinguished. The first detected change in polarization from the virgin state did not show any marked differences between the separate temperature ranges, I–IV, although an increase in the required poling field is seen

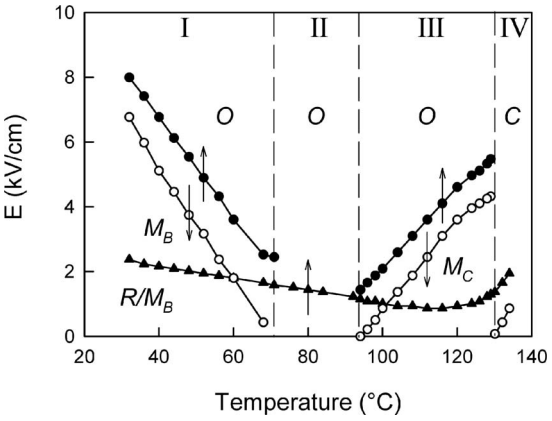

FIG. 5. Temperature dependence of threshold electric fields of induced polarization changes and proposed phase stability ranges in ⟨011⟩-oriented PMN-28PT. The first polarization changes from a depoled virgin state due to sample poling are depicted as black triangles. Black (white) circles indicate threshold fields with an increasing (decreasing) electric field, starting from a virgin state after zero-field cooling. The direction of the electric field is marked with arrows.

with increasing temperature in the vicinity of the depolarization temperature.

The temperature dependencies of the determined threshold electric fields in the field-induced reversible phase transitions (Fig. 5) are linear in temperature ranges I (32–68 °C) and III (96–129 °C). The difference is that in lower temperature range I the inducing field decreases, as found earlier in Ref. 51 while in higher temperature range III it increases with increasing temperature. The observed polarization behavior in temperature range III implies a different type of field-induced phase transition, which follows a different type of polarization rotation than in temperature range I. Cao *et al.*[31] actually found that for compositions with a higher PT content inside the MPB ($30<x\leq 35\%$ in PMN-xPT), the polarization rotation pathway with increasing E beginning from the ZFC condition is $M_C \rightarrow O$ instead of $R \rightarrow M_B \rightarrow O$ for $E \| [110]$. This phase transition is possibly present also in the studied PMN-28PT material, and as a difference, it appears here only at higher temperatures in region III, being responsible for the different polarization behavior in that temperature range. It is noteworthy that the M_C and O phases are closely linked to the presence of a stable T phase but the zero-field tetragonal phase reportedly was not found in ⟨110⟩-oriented compositions with a PT content below 30%.[31]

When moving to higher temperatures in range I, the inducing phase transition threshold field decreases, and finally the observed sudden change in polarization with an increasing field becomes indistinguishable from the first virgin polarization change, and the back-inducing threshold field for a reversible change diminishes to zero when entering temperature range II. Therefore, it seems that the crystal changes irreversibly into the orthorhombic phase upon application of a sufficiently strong electric field in range II. The virgin ground-state phase in region II after ZFC from 180 °C is either rhombohedral or tetragonal.

C. Field-induced temperature changes

The direct electrocaloric temperature changes induced by individual electric-field pulses from 9 to 1 kV/cm are shown as a function of temperature in Fig. 6. As in the case of polarization measurements, three distinct anomalies were identified in the temperature responses, and their temperature characteristics corresponded well with phase stability areas I–IV depicted in Figs. 2 and 5. The strongest temperature change of $\Delta T=0.53$ °C with $E=9$ kV/cm was achieved just above the crystal's depolarization temperature, and two other lower transitions were detected at 96 and 66 °C. Clearly different phases present in the different temperature areas provide their unique thermal response to the applied electric field. There is a drastic change with certain electric fields close to the transition regions just above temperatures 130 and 96 °C as well as just below 66 °C. Interestingly, the total electrocaloric temperature change changes temporarily to a negative value in a narrow temperature range below 66 °C.

A closer look at the field-induced temperature change behavior is taken in Fig. 7, where the induced temperature changes are expressed as a function of electric field in four

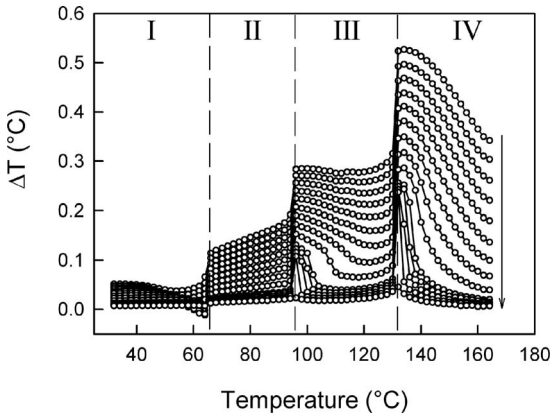

FIG. 6. Temperature dependence of electrocaloric temperature change curves in ⟨011⟩-oriented PMN-28PT with electric fields of 9–1.8 kV/cm (0.8 kV/cm decrements) and 1.6–1 kV/cm (0.2 kV/cm decrements). Temperature change was measured individually at each constant temperature for a series of electric-field pulses with decreasing strength. The direction of the decreasing electric field is marked with an arrow.

different temperature ranges: 31–71 °C (range I in Fig. 7), 73–97 °C (range II), 101–127 °C (range III), and 130–162 °C (range IV in the inset of Fig. 7), respectively. The behaviors of the two reversible phase transitions (ranges I and III) differ significantly from each other. When the electric field reaches a critical value in temperature range I, the crystal temperature decreases rapidly, whereas above 97 °C (range III) it conversely abruptly increases during field inducement. The critical field strengths extracted from these sudden changes are close to the ones determined in the polarization change measurements in Fig. 5. This indicates that the field-induced phase transitions are accompanied by abrupt thermal changes, which supports the fact that these transitions are first orderlike, involving latent heat. In addi-

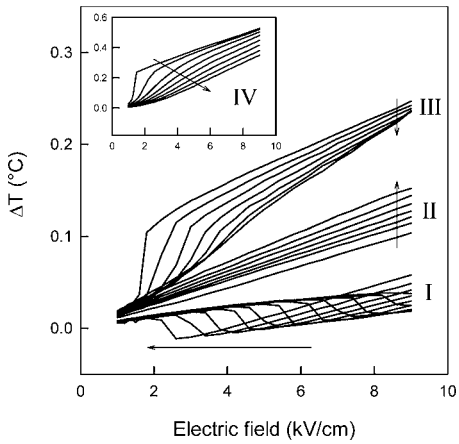

FIG. 7. Field-induced temperature change in ⟨011⟩-oriented PMN-28PT in the temperature ranges of (I) 31–71 °C, (II) 73–97 °C, and (III) 101–127 °C measured with descending field strengths. The inset shows the field-induced temperature change above the depolarization temperature in the temperature range of (IV) 134–162 °C. The direction of the increasing temperature is marked with arrows.

tion, an observed difference in the thermal behavior of the phase transitions further suggests that the field-induced phase transition above 94 °C in region III most likely involves a different phase sequence than the known $M_B \rightarrow O$ transition in region I. This means that after zero-field cooling from 180 °C, the crystal has a different kind of virgin ground state, at least in region III. As pointed out earlier, this reversible phase transition to the orthorhombic phase is possibly initiated from the monoclinic M_C phase originating from the tetragonal ground state.

However, when the polarization and temperature changes during the reversible phase transitions in temperature regions I and III were followed, it was discovered that the amount of hysteresis and induced abrupt change were both decreased when the required electric field for the phase transitions was increased; especially the abrupt temperature change in region III decreases rapidly, thus more resembling second-orderlike behavior. Interestingly, Viehland and Li[59] observed anhysteretic field-induced transformation behavior in ⟨110⟩-oriented PMN-30PT at room temperature, and this could indicate that there is a common trend toward decreasing hysteresis and possible second-orderlike transition behavior with an increasing field. Especially in temperature range III, the abrupt increase seen in the field-induced temperature at 99 °C (Fig. 7) smears out totally when moving toward the depolarization temperature. Similarly, above the depolarization temperature (region IV), the drastic increase in the field dependence of the temperature change smears out little by little with increasing temperature, turning into a more linear response, which at even higher temperatures starts to resemble exponential behavior with an increasing field, such as in ⟨110⟩-oriented PZN-PT.[63]

The nature of the previously observed field-induced reversible phase transitions in ⟨011⟩-oriented PMN-PT and PZN-PT has been quite unclear. Signs of first-order phase transitions, including hysteresis in the inducing field and/or abrupt changes in either polarization or strain in a certain field, have been evidenced during the $(R) \rightarrow M_B \rightarrow O$ phase transition in PMN-xPT (with $x=28$ and 30%) and PZN-4.5PT.[8,55–57] This means that the polarization rotation path must involve a drastic jump, and it cannot be totally continuous. In addition, Davis *et al.*[64] found by means of strain and polarized light microscopy that ⟨111⟩-oriented PZN-8PT exhibits a similar phase transition with a reversed path, namely, $O \rightarrow M_B \rightarrow R$, which showed first-orderlike transition characteristics. However, anhysteretic and more continuous phase transition behavior has also been observed in ⟨011⟩-oriented PMN-30PT (Ref. 59) and PMN-32 PT (Ref. 65). It has been proposed that the random fields present in complex perovskites due to B-site disorder can result in variation in threshold fields and thus more diffuse field-induced phase transition.[66] In this study, the polarization and temperature measurements at least partially imply first-orderlike $M_B \rightarrow O$ phase transition behavior in temperature range I with significant hysteresis and an abrupt temperature change.

In temperature region II (Fig. 7) between the two field-induced reversible phase transition temperature regions, I and III, the field-induced temperature change shows linear dependence on the electric field. In fact, the slope behavior of the linear dependence is in line with the dependence found in lower range I taken after the field-induced transition, where the orthorhombic phase is stable. And it seems that after initial polarization the crystal is in the orthorhombic state, which is then stable in temperature range II in the absence of an electric field.

Although the studied phase transitions in regions I and III are reversible in nature, it is evident that, like in relaxors in general, the electrical history and aging of the sample also play a significant role. This was especially evidenced when the electrocaloric temperature change was measured. Some variations in temperature between the different phase stability ranges I–IV were detected, depending on the measurement procedure and the crystal used. The polarization curves (Fig. 3) and individual temperature changes (Fig. 7) were recorded with intermediate depolarization annealing steps while the electrocaloric temperature change (Fig. 6) was measured sequentially at each temperature without depolarization. In particular, the temperature separating regions I and II varied considerably, having a lowest value of 64–66 °C in continuous electrocaloric measurement (Fig. 6) and a highest value of 71–73 °C in electrocaloric measurement with a depolarization step before each measured temperature point (Fig. 7). In the first case the sample was already polarized at the previous temperatures before the measurement while in the second measurement procedure the sample was in a depoled virgin state in the beginning of the measurement. Additionally, the polarization measurement was performed with a continuous electric field while the temperature responses were recorded separately for each electric-field strengths used. These differences in measurement procedures together with possible variance in composition between the single-crystal samples are believed to be the reason for the variation in the transition temperatures and threshold fields.

IV. SUMMARY

Electric-field-induced phase transitions were studied in a ⟨011⟩-oriented PMN-28PT single crystal by means of thermal and dielectric changes with electric fields up to 9 kV/cm. Dielectric changes were recorded as a form of permittivity and isothermal hysteresis loops with continuous field, and thermal changes were measured as a response to rectangular electric-field pulses with and without sequential annealing above the depolarization temperature. According to the observed anomalous changes in field-induced polarization and temperature, the studied temperature range formed four different temperature ranges, I–IV. These distinct temperature ranges with different phase stability characteristics are highlighted in Fig. 5.

In temperature range I the material exhibits uniform sharp changes in polarization and temperature after initial poling, and these changes are associated with a reversible field-induced $M_B \rightarrow O$ phase transition. During this phase transformation the temperature of the crystal decreased, which indicates absorbed heat energy in terms of endothermic behavior. In temperature range II the crystal is irreversibly transformed to the field-induced orthorhombic phase with increased rem-

anent polarization and decreased relative permittivity. This orthorhombic phase showed the linear field dependence of the induced temperature change. Temperature range III included another reversible field-induced phase transition that manifested itself with abrupt increases in field-induced temperature and polarization. The differences in comparison to the lower temperature $M_B \rightarrow O$ phase transition suggest that the phase transformation follows an alternative route, possibly $M_C \rightarrow O$. The ⟨011⟩-oriented PMN-28PT crystal changes to a cubic phase in temperature range IV above the depolarization temperature. In this range the electrocaloric temperature change has its maximum value of $\Delta T = 0.53$ °C with $E = 9$ kV/cm.

Both detected reversible phase transitions in regions I and III showed considerable hysteresis in the inducing threshold fields, and in higher electric fields, the magnitude of abrupt polarization and temperature changes due to reversible phase transitions was decreased, indicating a more continuous second-orderlike transition.

ACKNOWLEDGMENTS

Author J.P. gratefully acknowledges the Graduate School in Electronics, Telecommunications and Automation (GETA), the Foundation of Nokia Corporation, the Jenny and Antti Wihuri Foundation, the Tauno Tönning Foundation, the Ulla Tuominen Foundation, and the Riitta and Jorma J. Takanen Foundation for the financial support of the work.

[1] X.-h. Du, J. Zheng, U. Belegundu, and K. Uchino, Appl. Phys. Lett. **72**, 2421 (1998).
[2] D. V. Taylor and D. Damjanovic, Appl. Phys. Lett. **76**, 1615 (2000).
[3] J. Kuwata, K. Uchino, and S. Nomura, Jpn. J. Appl. Phys., Part 1 **21**, 1298 (1982).
[4] S.-E. Park and T. R. Shrout, J. Appl. Phys. **82**, 1804 (1997).
[5] B. Noheda, D. E. Cox, G. Shirane, J. A. Gonzalo, L. E. Cross, and S.-E. Park, Appl. Phys. Lett. **74**, 2059 (1999).
[6] G. Xu, H. Luo, H. Xu, and Z. Yin, Phys. Rev. B **64**, 020102 (2001).
[7] Z.-G. Ye, B. Noheda, M. Dong, D. Cox, and G. Shirane, Phys. Rev. B **64**, 184114 (2001).
[8] H. Cao, F. Bai, N. Wang, J. Li, D. Viehland, G. Xu, and G. Shirane, Phys. Rev. B **72**, 064104 (2005).
[9] J.-M. Kiat, Y. Uesu, B. Dkhil, M. Matsuda, C. Malibert, and G. Calvarin, Phys. Rev. B **65**, 064106 (2002).
[10] D. Vanderbilt and M. H. Cohen, Phys. Rev. B **63**, 094108 (2001).
[11] L. Bellaiche, A. Garcia, and D. Vanderbilt, Phys. Rev. Lett. **84**, 5427 (2000).
[12] B. Noheda, Curr. Opin. Solid State Mater. Sci. **6**, 27 (2002).
[13] H. Fu and R. E. Cohen, Nature (London) **403**, 281 (2000).
[14] B. Noheda and D. E. Cox, Phase Transitions **79**, 5 (2006).
[15] E. H. Kisi, R. O. Piltz, J. S. Forrester, and C. J. Howard, J. Phys.: Condens. Matter **15**, 3631 (2003).
[16] J. Frantti, Y. Fujioka, and R. M. Nieminen, J. Phys.: Condens. Matter **20**, 472203 (2008).
[17] M. Davis, J. Electroceram. **19**, 25 (2007).
[18] D. Hatch, H. T. Stokes, and W. Cao, J. Appl. Phys. **94**, 5220 (2003).
[19] M. Davis, D. Damjanovic, and N. Setter, Phys. Rev. B **73**, 014115 (2006).
[20] Y. U. Wang, Phys. Rev. B **74**, 104109 (2006).
[21] Y. U. Wang, Phys. Rev. B **76**, 024108 (2007).
[22] Z. Xu, M. Kim, J. Li, and D. Viehland, Philos. Mag. A **74**, 395 (1996).
[23] Y. M. Jin, Y. U. Wang, A. G. Khachaturyan, J. F. Li, and D. Viehland, J. Appl. Phys. **94**, 3629 (2003).
[24] Y. M. Jin, Y. U. Wang, A. G. Khachaturyan, J. F. Li, and D. Viehland, Phys. Rev. Lett. **91**, 197601 (2003).
[25] H. Wang, J. Zhu, X. W. Zhang, Y. X. Tang, and H. S. Luo, Appl. Phys. Lett. **92**, 132906 (2008).
[26] R. R. Chien, V. H. Schmidt, C.-S. Tu, and F.-T. Wang, J. Appl. Phys. **98**, 114106 (2005).
[27] P. Bao, F. Yan, X. Lu, J. Zhu, H. Shen, Y. Wang, and H. Luo, Appl. Phys. Lett. **88**, 092905 (2006).
[28] Z.-G. Ye and M. Dong, J. Appl. Phys. **87**, 2312 (2000).
[29] V. V. Shvartsman and A. L. Kholkin, Phys. Rev. B **69**, 014102 (2004).
[30] A. J. Bell, J. Appl. Phys. **89**, 3907 (2001).
[31] H. Cao, J. Li, D. Viehland, and G. Xu, Phys. Rev. B **73**, 184110 (2006).
[32] V. Bobnar, Z. Kutnjak, R. Pirc, and A. Levstik, Phys. Rev. B **60**, 6420 (1999).
[33] Z. Kutnjak, B. Vodopivec, and R. Blinc, Phys. Rev. B **77**, 054102 (2008).
[34] J. Peräntie, J. Hagberg, A. Uusimäki, and H. Jantunen, Appl. Phys. Lett. **93**, 132905 (2008).
[35] F. Bai, N. Wang, J. Li, D. Viehland, P. M. Gehring, G. Xu, and G. Shirane, J. Appl. Phys. **96**, 1620 (2004).
[36] B. Noheda, Z. Zhong, D. E. Cox, G. Shirane, S.-E. Park, and P. Rehrig, Phys. Rev. B **65**, 224101 (2002).
[37] Y. Lu, D.-Y. Jeong, Z. Y. Cheng, Q. M. Zhang, H. S. Luo, Z. W. Yin, and D. Viehland, Appl. Phys. Lett. **78**, 3109 (2001).
[38] D. Viehland, A. Amin, and J. F. Li, Appl. Phys. Lett. **79**, 1006 (2001).
[39] B. A. Tuttle and D. A. Payne, Ferroelectrics **37**, 603 (1981).
[40] J. Peräntie, J. Hagberg, A. Uusimäki, and H. Jantunen, Appl. Phys. Lett. **94**, 102903 (2009).
[41] A. S. Mischenko, Q. Zhang, R. W. Whatmore, J. F. Scott, and N. D. Mathur, Appl. Phys. Lett. **89**, 242912 (2006).
[42] B. Neese, B. Chu, S.-G. Lu, Y. Wang, E. Furman, and Q. Zhang, Science **321**, 821 (2008).
[43] D. Q. Xiao, Y. C. Wang, R. L. Zhang, S. Q. Peng, J. G. Zhu, and B. Yang, Mater. Chem. Phys. **57**, 182 (1998).
[44] L. Shaobo and L. Yanqiu, Mater. Sci. Eng., B **113**, 46 (2004).
[45] G. Sebald, L. Seveyrat, D. Guyomar, L. Lebrun, B. Guiffard, and S. Pruvost, J. Appl. Phys. **100**, 124112 (2006).
[46] O. Noblanc, P. Gaucher, and G. Calvarin, J. Appl. Phys. **79**,

4291 (1996).
[47] E. V. Colla, N. K. Yushin, and D. Viehland, J. Appl. Phys. **83**, 3298 (1998).
[48] M. Davis, Ph.D. thesis, École Polytechnique Fédérale de Lausanne, 2006.
[49] K. K. Rajan, M. Shanthi, W. S. Chang, J. Jin, and L. C. Lim, Sens. Actuators, A **133**, 110 (2007).
[50] C.-S. Tu, V. H. Schmidt, R. R. Chien, S.-H. Tsai, S.-C. Lee, and H. Luo, J. Appl. Phys. **104**, 094105 (2008).
[51] T. Liu and C. S. Lynch, Continuum Mech. Thermodyn. **18**, 119 (2006).
[52] Y. Guo, H. Luo, H. Xu, X. Zhou, X. Pan, and Z. Yin, Appl. Phys. A: Mater. Sci. Process. **77**, 707 (2003).
[53] Z. Feng, X. Zhao, and H. Luo, J. Appl. Phys. **100**, 024104 (2006).
[54] D. Zekria, V. A. Shuvaeva, and A. M. Glazer, J. Phys.: Condens. Matter **17**, 1593 (2005).
[55] Z. Feng, H. Luo, Y. Guo, T. He, and H. Xu, Solid State Commun. **126**, 347 (2003).
[56] M. Shanthi and L. C. Lim, J. Appl. Phys. **106**, 114116 (2009).
[57] T. Liu and C. S. Lynch, Acta Mater. **51**, 407 (2003).
[58] M. Shanthi, S. M. Chia, and L. C. Lim, Appl. Phys. Lett. **87**, 202902 (2005).
[59] D. Viehland and J. F. Li, J. Appl. Phys. **92**, 7690 (2002).
[60] J. Yao, H. Cao, W. Ge, J. Li, and D. Viehland, Appl. Phys. Lett. **95**, 052905 (2009).
[61] H. Wang, H. Xu, H. Luo, Z. Yin, A. A. Bokov, and Z.-G. Ye, Appl. Phys. Lett. **87**, 012904 (2005).
[62] F. Chu, I. M. Reaney, and N. Setter, J. Appl. Phys. **77**, 1671 (1995).
[63] M. Valant, L. J. Dunne, A.-K. Axelsson, Neil McN. Alford, G. Manos, J. Peräntie, J. Hagberg, H. Jantunen, and A. Dabkowski, Phys. Rev. B **81**, 214110 (2010).
[64] M. Davis, D. Damjanovic, and N. Setter, J. Appl. Phys. **97**, 064101 (2005).
[65] E. A. McLaughlin, T. Liu, and C. S. Lynch, Acta Mater. **52**, 3849 (2004).
[66] A. J. Bell, Appl. Phys. Lett. **76**, 109 (2000).